

## Mechanical and Tribological Behaviours of Aluminium Metal Matrix Composite Reinforced with Bamboo Powder and Iron Filings



Omolayo M. Ikumapayi<sup>1,2,3\*</sup>, Opeyeolu T. Laseinde<sup>1</sup>, Tin T. Ting<sup>3</sup>

<sup>1</sup> Department of Mechanical and Industrial Engineering, University of Johannesburg, Johannesburg 2092, South Africa

<sup>2</sup> Department of Mechanical and Mechatronics Engineering, Afe Babalola University, Ado Ekiti 360101, Nigeria

<sup>3</sup> Faculty of Data Science and Information Technology, INTI International University, Nilai 71800, Malaysia

Corresponding Author Email: [ikumapayi.omolayo@gmail.com](mailto:ikumapayi.omolayo@gmail.com)

Copyright: ©2024 The authors. This article is published by IIETA and is licensed under the CC BY 4.0 license (<http://creativecommons.org/licenses/by/4.0/>).

<https://doi.org/10.18280/rcma.340406>

### ABSTRACT

**Received:** 25 February 2024

**Revised:** 4 May 2024

**Accepted:** 10 June 2024

**Available online:** 27 August 2024

#### Keywords:

Aluminium 6061, iron fillings, bamboo powder, reinforcement, composite, metal matrix composite, stir casting

Metal Matrix Composites have wide range of applications in different industries. Conventional materials have limitations when compared to composite materials as they may be lacking in some properties. Metal matrix composites, in particular, offer significant potential because of their improved mechanical and tribological characteristics such as tensile strength, hardness, toughness, and wear resistance. The research aims to produce aluminium 6061 metal matrix composites by incorporating bamboo powder and iron fillings as reinforcements, by so doing, SDG targets 9 and 11 will be met. An efficient and economical approach for producing the composites is crucial. The reinforcement can be readily included into the melt utilizing the cost-effective and readily accessible stir casting procedure. Hardness test, wear test, and impact strength tests were conducted on samples produced using the stir casting technique for comparison. From the results, sample 4 (15% iron fillings) had the highest hardness number value and impact energy value and had the lowest wear rate value. Then sample 1 (15% bamboo powder) gave the least impact energy value. Sample 5 (control) gave the least hardness number value followed by sample 1 (15% bamboo powder). Lastly, sample 2 (5% iron fillings and 10% bamboo powder) gave the highest wear rate and sample 4 (15% iron fillings) had the least wear rate value, meaning it has the highest wear resistance value. The result obtained will be useful in the interdisciplinary fields such as materials science, mechanical engineering and structural engineering as well as materials sustainability.

## 1. INTRODUCTION

Aluminium as a metal is widely known and is generally referred to as the most plentiful metal type in the world, taking account for 8 percent of total of the crust of the earth (by weight). Because of its convenient machinability and surface quality finish, as well as exceptional thermal and electrical conductivities, this nonferrous metal with such a density of 2.7g/cm<sup>3</sup> has a broad spectrum of potential uses [1]. Aluminium is recovered from a parent material known as bauxite ore via a known process called “Bayer process”. Aluminium trihydrate is solubilized during the purification process, putting titanium oxide and iron as byproducts.

Aluminium metal composites are advanced lightweight aluminium material systems known for their outstanding qualities. AMC strengthening can take the form of continuous or discontinuous fibers, whiskers, or particles. By combining appropriate matrix, conditioning, and processing route combinations, AMC features can be customized to meet the requirements of many different industrial uses [2]. Many different types of AMCs are manufactured [3]. Stiffness and strength are provided by the reinforcing stage. The

reinforcement is usually tougher, stronger, and more rigid than the matrix. Typically, particles reinforced epoxy materials have very little reinforcement due to manufacturing issues and brittleness (up to 40 to 50 volume percent).

On a microscale, a composite is a blend of a number of distinct elements or phases, differentiated by a sharp distinction, and have a well-defined interface. In addition, other conditions must usually be met before a metal can be labelled as a composite [4]. The components must be present in sufficient quantities, and the constituting stages must have notably different properties, such that the composite's properties are clearly distinct from either the constituents' characteristics [3]. The matrix is the continuous constituent that is usually available in higher amounts. It is often assumed that the characteristics of the matrix are improved during the composite production process. The second ingredient is termed as that of the reinforcement material, or reinforcement, because that improves or strengthens the matrix's mechanical characteristics [4, 5]. The matrix seems to be formed of metallic, ceramic or polymeric components, each of which has radically distinct/unique mechanical characteristics. Polymers, in general, have lower strengths; ceramics have reduced

stiffness, toughness, and brittleness; while metals possess advanced moduli, strengths, and ductility [6].

Various materials have been used by researchers to reinforce aluminium matrix composites. Among them are ceramics, nitrides, metal alloys, and agricultural waste products. In addition, there have been indications on how the mechanical and structural properties of composites produced differ based on the kind of structural support utilised, as distinct interphases resurface in the composite. Chemical or mechanical interfacial bonding occurs frequently when matrix and reinforcements come into contact. Nonetheless, bonding management is critical for optimizing diffusion response and improving interface properties [4, 6].

Composite materials are typically classed based on the physical or chemical characteristics of the matrix, for example, metal matrix, polymer matrix, and ceramic composites. Furthermore, as noted by Cheng et al. [7], the emergence of intermetallic matrix and carbon composite material has widened the scope of composites. Metallic compounds, such as TiAl, Nb<sub>3</sub>Al, Ni<sub>3</sub>Al, and Ti<sub>3</sub>Al, are compounds focused on the atomic quantities that are fixed and available in the form of metals alloys made from aluminium with titanium (Ti), niobium (Nb). Intermetallic compounds are of importance because the lattice structure of their atoms causes them to have higher melting temperatures and less deformation [4-8]. Titanium carbide (TiC), silicon carbide (SiC), and boron carbide (B<sub>4</sub>C) have surfaced as feasible reinforcement substances for the creation of aluminium matrix composites due to their intrinsic mechanical properties. The composites that arise are employed in applications that need great strength and stiffness. A unidimensional aluminium metal matrix composite with carbide fiber reinforcements was created using melt infiltration, a one-step pressure less method, with bonds are formed between both the matrices and carbide reinforcements. Factors such as holding duration, processing method, matrix composition and processing temperature were discovered to have an effect on this created interface bond [9, 10].

Hybrid MMCs are made up of more than one form of reinforcement, such as a blend of particle and whisker, a blend of fiber and particle, or a blend of hard and soft supports. Carbon nanotubes (CNT) discovery has resulted in composites with greater tensile characteristics than carbon [9]. Metal matrix composite (MMCs) have reinforcements with aspect ratios above 5, although they are not consistent. Short Al<sub>2</sub>O<sub>3</sub> fiber-supported MMCs have traditionally been employed in pistons. Using powder metallurgy or squeezing infiltration into a fiber preform, whisker-reinforced composites are typically manufactured in net/near-net shape. However, because of health hazards, by use of whiskers as reinforcement material has become prohibited [4].

A stirring method facilitates reinforcing atoms or short fibres into a lava or semi-solid metal matrix during the process of metal-liquid mixing. The stir casting technique entails incorporating ceramic particles into liquid aluminium melt and then solidifying the mixture. Sufficient wettability in between particle structural support and the liquid aluminium melt is critical. Particles of ceramic ranging from sizes 5m to 100m can be incorporated into the wide range of molten aluminium alloys [4]. Surappa [3] describes compo-casting, a type of stir casting technique in which ceramic materials are presented into the composite material while it is still semi-solid. Since the 1990s, particle-reinforced AlMMCs have been widely available on the market. The combination of high physic

mechanical qualities provided through the aid of reinforcement despite the retention of the advantageous working on the metal attributes and largely metal-like behaviour piqued the interest of researchers in these MMCs. Another factor that motivates is the possibility of modification of both the physical and mechanical properties by selecting the reinforcement composition alloy.

The mechanical properties of aluminium matrix composites are determined by factors such as reinforcement size and shape, stirring period, processing temperature and reinforcement distribution in the metal matrix [10]. The effect of these factors on mechanical qualities such as toughness, tensile strength, and tribological properties of manufactured composites is addressed in detail [1].

Krishnan et al. [11] investigated the microstructural integrity and carried out a mechanical analysis of aluminium-based Metal Matrix Composites derived from waste metal and hybrid material parts. As matrix materials, AlSi7Mg alloy billets and waste aluminium were used, with 50m particle size aluminium and waste aluminium catalyst provided locally using a crude oil refinery acting as support. Matrices of aluminium composites were created via an adoption of the squeeze casting process. The matrix composite packing temperature was 3000 degrees Celsius, then raised to 7500 degrees Celsius to allow complete melting of charged aluminium. Magnesium was added before the reinforcements to guarantee permeability of the reinforcement and its matrix. Table 1 displays the parameters used in the squeeze casting of composites. The polymer made of AlSi7Mg and aluminium reinforcing steel had the highest recorded tensile strength of 172MPa, yield stress of 53MPa, durability to rupture value of 4.6%, and rupture stress of 171MPa, while scrap aluminium and aluminium oxide had 37.3MPa, ultimate tensile of 125MPa, elasticity to fracture value of 2.7%.

**Table 1.** Composite squeeze casting process parameters

S/N	Process Parameter	Value
1	Speed for Stirring	650rev/min
2	Temperature for Stirring	750°C
3	Time taken for Stirring	10 minutes
4	Reinforcement temperature of particles before heating	300°C
5	Pressure of Squeeze	200MPa
6	Temperature of permanent die before heating	300°C

### 1.1 Reinforcements made from agrobased materials

Agro-based products (agricultural resources) has always been very important to the men of the early days because of their widespread use in the construction of equipment, firearms, and shelters due to their multi-purpose, aesthetic, and regenerative properties. Due to the high density and cost of manufacturing aluminium matrix composites with ceramic grains as reinforcements, several scientists have used agro-based materials such as fly ash, coconut husk, bamboo leaves, and ash from rice husks instead of ceramic particles. Fly ash is used as reinforcement in aluminium matrices due to its low density and low procurement cost. Nevertheless, fly ash, a byproduct of coal combustion, can be categorized as either a sedimentation tanks or a cenosphere. The cenosphere fly ash is made up of hollow particles with a density of around 1.0 g/cm<sup>3</sup>, meanwhile the pressurizer fly ash has a range of concentrations of 2-2.5 g/cm<sup>3</sup> and enhances properties like strength, wear resistance, and stiffness by lowering the density

of chosen matrix components. Rice husk is a farm product that is widely available all over the world. The burned rice husk vaporizes the volatile substance and transforms it to ash. Rice husk ash is regarded as a cost-effective ceramic reinforcement when compared to other ceramic reinforcements [9, 10].

The incorporation of bamboo fibers enhances the strength, stiffness, and durability of the composite material. The thermoplastic polymer matrix functions as a cohesive agent that binds the bamboo fibers together and imparts the composite with its specific shape and structure [8, 9, 11].

## 2. MATERIALS AND METHODS

### 2.1 Materials

#### 2.1.1 Base material

Aluminium alloy 6061 was used in this research with the following chemical compositions Al (95.03%), Mn (0.14%), Si (0.34%), Mg (1.17%), Fe (0.46%), and Cu (0.15%). About 2000 g of this aluminium billet was purchased. The chemical composition of the alloy is shown in Table 2. Other materials used in this study are iron fillings of about 150 g and bamboo powder of about 420 g. The quantity of each of the materials is presented in Table 3 and Figure 1 shows aluminium billet.

**Table 2.** Chemical composition of 6061 aluminium alloy

Element	Al	Mn	Si	Mg	Fe	Cu	Others
Composition (%)	95.03	0.14	0.34	1.17	0.46	0.15	2.71



**Figure 1.** Aluminium billet

#### 2.1.2 Reinforcement material

##### Iron fillings material preparation

The 150 g of iron fillings purchased was used as reinforcement. It was grounded and sieved to a finer particle using a 425, and 150-micrometre sieve mesh. The iron fillings were then measured as indicated in Figure 2 and divided into three parts with different masses (g), according to the mixing ratio.

##### a. Bamboo powder preparation

The 420 g bamboo was carburized. The resulting product weighed 300 g, and this contained carburized bamboo powder and charcoal residue. The carburized bamboo powder was manually separated from the charcoal residue, before pouring it into a sieving pan shown in Figures 3(a) and (b), respectively to get finer particles. 170 g of the fine bamboo powder was measured using a measuring scale. The bamboo powder was

separated into different masses according to the desired mixing ratio for the composite preparation. Bamboo powders (BP) (length, - 200m, diameter, 10-35  $\mu$ m).



**Figure 2.** Measurement of iron filings

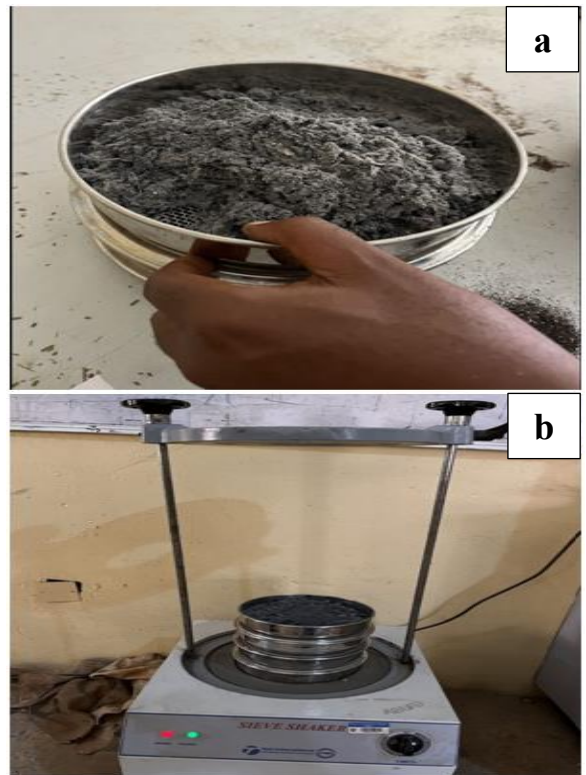


**Figure 3.** Carburized bamboo powder: (a) in a sieve pan; (b) in a sieve shaker

## 2.2 Materials preparation

The sample preparation involves cleaning the aluminium billets to remove any form of impurity. Most of the sandy impurities and dirt were removed from the aluminium AA6061 billets using emery cloths. The iron fillings material and the bamboo powder were also prepared prior to the stir casting process.

### 2.3 Methods

#### 2.3.1 Preparation of aluminium matrix composites

The iron fillings and bamboo powder were added to aluminium AA6061 to prepare the metal matrix composite using a stir casting technique. Table 1 displays the casting/stirring parameters adopted. Table 3 shows the mixing

ratio of the reinforcements and the base metal. Sample S<sub>1</sub> has the highest percentage composition of bamboo powder, while

the S<sub>4</sub> sample has the highest percentage composition of iron fillings.

**Table 3.** Mixing ratio of AA6061 to reinforcements (iron fillings and bamboo powder)

Sample	Mass Fraction of Al (g)	Reinforcement Fraction (Iron Fillings)		Reinforcement Fraction (Bamboo Powder)		Mass of Composite (g)
		Mass (g)	%	Mass (g)	%	
S <sub>1</sub>	294.70	----	----	50.25	15	344.95
S <sub>2</sub>	337.00	16.85	5	33.70	10	387.55
S <sub>3</sub>	280.36	34.30	10	17.15	5	331.81
S <sub>4</sub>	312.05	57.00	15	----	----	369.05
S <sub>c</sub>	381.56	----	----	----	----	381.56

### 2.3.2 Production of aluminium matrix composites

The aluminium billets were divided into five (5) portions, measured with a sensitive weighing balance and labelled as samples S<sub>1</sub>, S<sub>2</sub>, S<sub>3</sub>, S<sub>4</sub>, and S<sub>c</sub> (control sample) as shown in Table 3. Each billet portion was first preheated to 450°C to enable the addition of the modified bamboo/iron-filling powders before being finally melted at 750°C in a crucible furnace. During the liquefaction process, the mixture was thoroughly stirred at a stirring rate of 180rpm for 10 minutes. The liquid metal mixture was then poured into cylindrical moulds of dimensions 20 mm×300 mm. It was allowed to solidify at room temperature (See Figure 4). The solidified samples were thereafter removed from the mould, polished, machined and cut into smaller pieces (10 mm×10 mm) for characterization. The cross-section of the polished and machined aluminium composite produced.



**Figure 4.** Casted aluminium (AA6061) matrix composite

### 2.4 Mechanical testing of the composite: Impact test

A Charpy Impact test was conducted on the specimen with an ATICO Charpy tester following the ASTM E23 standard. The specimen had dimensions of 55 mm in length and 10 mm in width. A 45° V-notch, 2 mm deep with a 0.25 mm root radius, was created at the center of each specimen. The specimen was cleaned and positioned in the vice of an impact testing equipment with the notch at the center and supporting the hammer. The pendulum was elevated to its secured configuration at a pre-swing angle of 160°. The trajectory of the pendulum has been established and ensured all safety guards are in place. The scale pointer was reset to its default position and safety protocols were examined. The pendulum was released using the release mechanism to strike the specimen at the center, and the absorbed impact energy, E<sub>1</sub> (in joules) was recorded immediately from the scale. The experiment was replicated with the second and third specimens, E<sub>2</sub> and E<sub>3</sub> and the average value was taken and

recorded using Eq. (1). Then the impact strength was then computed using Eq. (2). The procedures were repeated for other specimens S<sub>2</sub>, S<sub>3</sub>, S<sub>4</sub> and S<sub>c</sub>.

$$\text{AvgIE} = \frac{E_1 + E_2}{2} \quad (1)$$

$$\text{IS} = \text{AvgIE} / A \quad (2)$$

### 2.5 Hardness test

Brinell hardness test was performed on the sample using an ATICO Brinell Hardness Tester in accordance to ASTM E10 standard. The load selector was set to 980 N. Each sample was carried out in triplicate to ensure reproducibility and the average value was recorded.

The specimen was polished cleaned to remove all dirt, grease and impurities it was placed on the anvil while making contact with the carbide ball indenter a 100KgF was applied at a dwell time of 30 seconds before unloading. The indentation procedure was followed for other parts of the specimen the indentation size is then measured using an optical microscope. Two consecutive readings were taken for each sample. The average indentation size (d) was calculated using the Eq. (3).

$$d = \frac{d_1 + d_2}{2} \quad (3)$$

The procedure was repeated for specimens S<sub>2</sub>, S<sub>3</sub>, S<sub>4</sub> and S<sub>c</sub>. The Brinell hardness was then calculated and recorded.

### 2.6 Wear test

The specimen's wear parameters were analyzed using a Rtec Universal Tribometer MTF 5000. The test piece measures 24 mm in length, 10 mm in width, and 6 mm in height.

The experiments followed ASTM G133-05 standards and utilized a cyclic wear test mode using E52100 alloy steel balls of grade 25 with a diameter of 6.35 mm. The surface of each sample experienced a 20N force while moving at a speed of 3 mm/s across a distance of 3 mm. The tribometer's microscope was utilized to capture photographs of the wear patterns. The data for analysis were acquired using the MFT17 software installed on the PC linked to the Rtec Universal tribometer. The MFT17 program was utilized to determine the coefficient of friction (COF), wear volume, friction force, and other properties for all the samples evaluated. The studies were conducted at a temperature of 25°C.

### 3. RESULTS AND DISCUSSION

#### 3.1 Analysis of impact test performed on bamboo powder/iron fillings reinforced AA 6061

The impact test performed on the composite formulated is presented in Table 4. The sample with the lowest impact strength is S<sub>1</sub> which contains 15% of bamboo reinforced AA 6061 indicating that the bamboo reinforcements didn't increase the impact strength of the AA 6061 rather it reduced the impact. Whereas samples S<sub>2</sub> containing 10% bamboo powder, 5% iron fillings reinforced AA6061, S<sub>3</sub> (5% bamboo

powder, 10% iron fillings reinforced AA6061), and S<sub>4</sub> (15% iron fillings reinforced AA6061) had more impact strength than the control. The impact strength of these reinforced AA6061 increased the impact more than normal with S<sub>4</sub> having the highest impact strength readings because of its higher percentage of iron fillings (15%).

Using the data shown in Table 5, the bar chart was plotted having impact in the Y-axis against the samples of the reinforced AA 6061 composite matrix on the X-axis as shown in Figure 5. The chart shows which sample has the highest impact strength and compare the reinforced samples (S<sub>1</sub>, S<sub>2</sub>, S<sub>3</sub>, and S<sub>4</sub>) with the control which is the S<sub>5</sub>.

**Table 4.** Impact Test data recorded from the experiment

Samples	a (Joules)	b (Joules)	c (Joules)	IE (J)	A (m <sup>2</sup> )	IE/A
S <sub>1</sub>	226	230	234	230	149	1.543624
S <sub>2</sub>	230	244	248	240.6667	149	1.615213
S <sub>3</sub>	262	265	265	264	150	1.76
S <sub>4</sub>	273	282	279	278	149	1.865772
S <sub>5</sub>	239	234	237	236.6667	151	1.567329

**Table 5.** Hardness test performed on the reinforced aluminium composite matrix

Sample	F	D	d1	d2	Davg	BHN
S <sub>1</sub>	218	10	1.8	1.55	1.675	98.22046
S <sub>2</sub>	218	10	1.7	1.6	1.65	101.2409
S <sub>3</sub>	218	10	1.6	1.6	1.6	107.7119
S <sub>4</sub>	218	10	1.6	1.5	1.55	114.8192
S <sub>5</sub>	218	10	1.8	1.6	1.7	95.33231

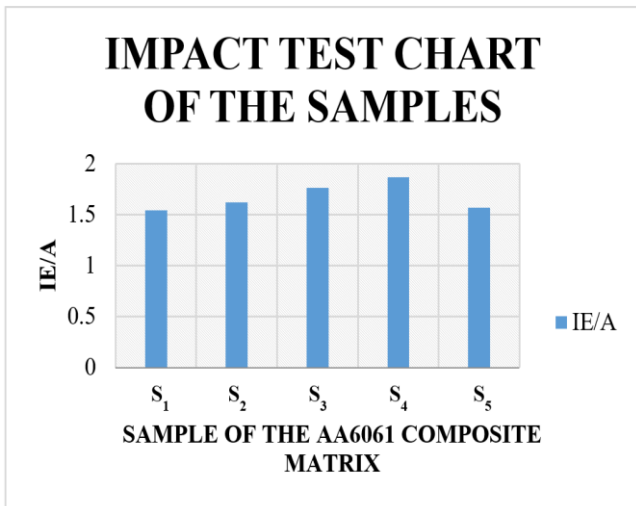


**Figure 5.** The graph chart for the impact of the reinforced AA 6061 composite matrix

number for AA6061 is 95.

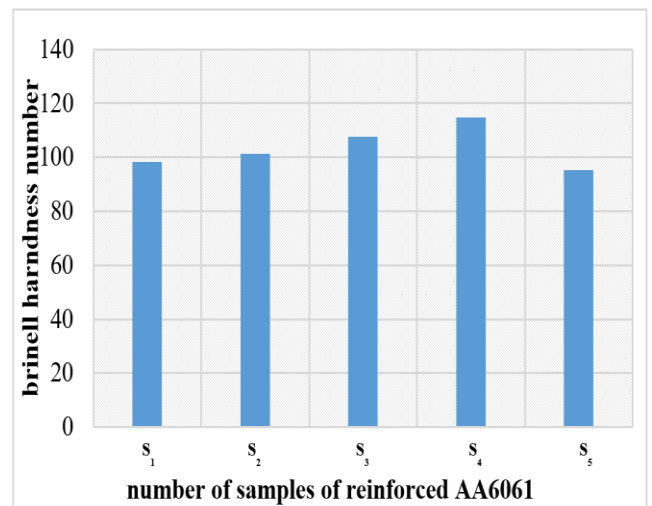


**Figure 6.** Brinell hardness test chart

#### 3.2 Analysis of hardness brinell hardness test of bamboo powder/ iron fillings reinforced AA 6061

The result of hardness test performed on the composite material is presented in Table 5.

Using the data shown in Table 5, the graph or bar chart was plotted having the brinell hardness number on Y-axis against the samples of the reinforced AA6061 composite matrix on the X-axis as shown in Figure 6. The chart shows which sample has the highest and lowest brinell hardness number and compare the reinforced samples (S<sub>1</sub>, S<sub>2</sub>, S<sub>3</sub>, and S<sub>4</sub>) with the control which is the S<sub>5</sub>. The control is the AA6061 without any reinforcements so the brinell hardness number was found to be 95.33 whereas the general brinell hardness

As shown in Figure 6, the sample with the lowest brinell hardness number is S<sub>5</sub> which is the control, AA 6061 without reinforcements which shows that the other samples S<sub>1</sub> (15% of bamboo reinforced AA 6061), S<sub>2</sub> (10% bamboo powder, 5% iron fillings reinforced AA6061), S<sub>3</sub> (5% bamboo powder, 10% iron fillings reinforced AA6061), and S<sub>4</sub> (15% iron fillings reinforced AA6061) had more the brinell hardness number than the control. the brinell hardness number of these reinforced AA6061 increased the hardness of the material with S<sub>4</sub> having the highest brinell hardness number readings which shows that the iron fillings increased the brinell hardness number or hardness of the AA6061 when reinforced with the 15% of iron fillings as shown in Figure 6.

### 3.3 Wear results SEM test results

Table 6 shows the results obtained from wear test carried out on the casted samples with different reinforcements. The following wear properties were investigated: wear volume or volume loss, wear resistance, wear rate, frictional force as well as coefficient of friction as depicted in Table 6. The wear test was conducted with an applied load of 20N, sliding distance of 3mm, sliding speed of 3 mm/s and sliding time of 5 minutes per sample. Each experiment was conducted at an ambient temperature of 25°C. During the wear test experiment, the wear width was obtained in the triplicate per sample and an average was taking for each sample as seen in Figures 7-11 and recorded in Table 6. Eqs. (4)-(8) were adopted in calculating wear parameters [12-18].

$$V_w = \frac{C_w dL}{3h} \quad (4)$$

where,

$C_w$  = Wear Coefficient,  
 $L$  = Load applied and  $V_w$  = Wear Volume,  
 $h$  = Substrate bulk hardness  
 $d$  = Sliding distance,

$$Volumeloss (mm^3) = \left( \frac{Weight\ loss \cdot (g)}{Density \left( \frac{g}{mm^3} \right)} \right) \times 1000 \quad (5)$$

$$Wear\ rate (mm^3/m) = \left( \frac{Volume\ loss (mm^3)}{Sliding\ distance (m)} \right) \times 1000 \quad (6)$$

$$Wear\ resistance (m/mm^3) = \left( \frac{Sliding\ distance (m)}{Volume\ loss (mm^3)} \right) \times 1000 \quad (7)$$

$$Coefficient\ of\ friction (\mu) = \frac{Friction\ Force (F_f)}{Applied\ Load (L)} \quad (8)$$

**Table 6.** Wear tests analysis conducted at room temperature

Parameters	20 N, 3 mm and 3 mm/s					
	Wear Rate (mm <sup>3</sup> /m)	Friction Force (N)	Wear Volume (mm <sup>3</sup> )	Wear Width (μm)	Wear Resistance (m/mm <sup>3</sup> )	COF
S <sub>1</sub>	14100	9.014	0.0423	1146.97	70.90	0.4507
S <sub>2</sub>	24200	9.818	0.0726	517.58	41.30	0.4909
S <sub>3</sub>	19500	9.322	0.0585	963.38	51.30	0.4661
S <sub>4</sub>	11333	9.002	0.0340	1093.23	88.20	0.4501
S <sub>c</sub>	16633	9.360	0.0499	1099.76	60.10	0.4680

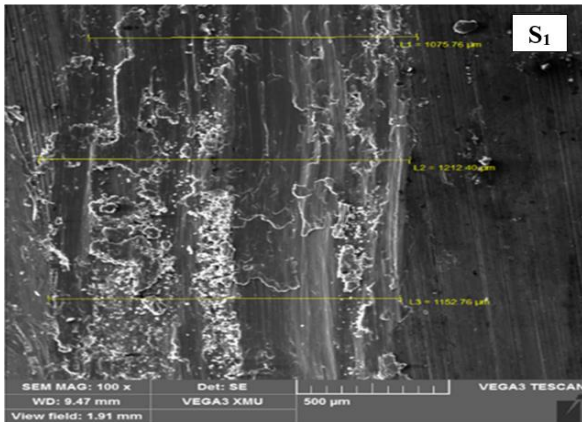


**Figure 7.** Morphology of Wear Track for speciment S<sub>1</sub>

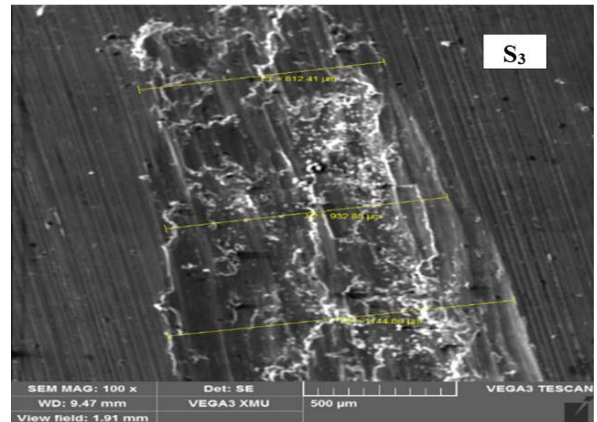


**Figure 9.** Morphology of Wear Track for speciment S<sub>3</sub>

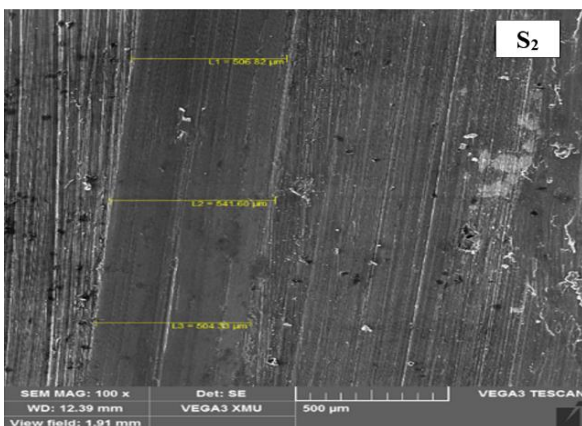


**Figure 8.** Morphology of Wear Track for speciment S<sub>2</sub>

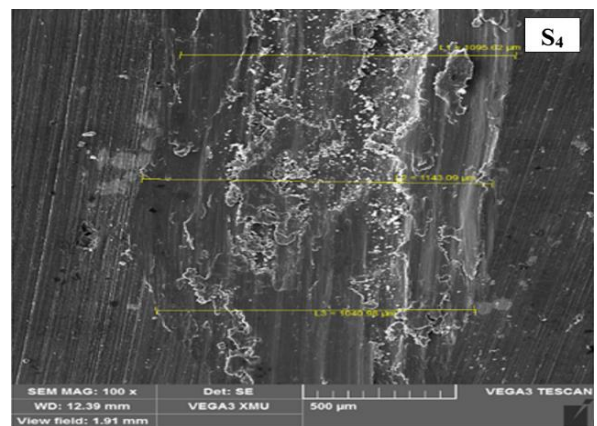


**Figure 10.** Morphology of Wear Track for speciment S<sub>4</sub>

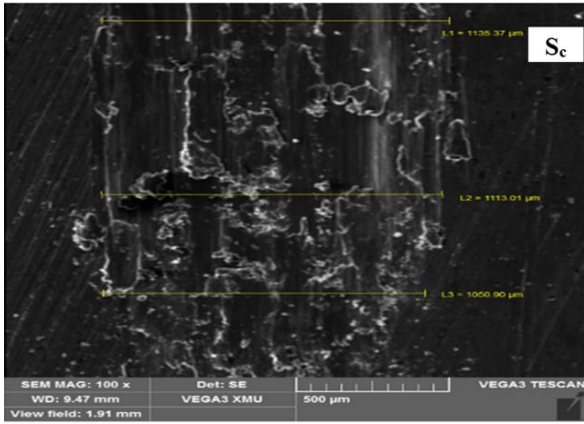


**Figure 11.** Morphology of Wear Track for specimen  $S_c$

Figures 7-11 exhibit significant debris present during morphological evaluation when a 20 N load was applied. This debris is likely a result of high heat produced during the sliding movement of the steel ball on the workpiece, leading to degradation of the material's properties through deformation caused by plastic and softening of wear paths. Consequently, wear debris accumulates along the wear track. It was observed that  $S_1$  sample had an average width of 1146.97  $\mu\text{m}$  being the widest while  $S_2$  had an average width of 517.58  $\mu\text{m}$  resulting to the least wear track [16, 19, 20].

Figure 12 represents wear rate for fabricated samples as well as the control sample. It was revealed that  $S_2$  had the highest wear rate which is the sample with (10% bamboo +5% iron filling) whereas samples  $S_4$  had the least wear rate which is the sample with (15% iron-filling reinforcement). It was further noticed that the wear rate between  $S_1$  and  $S_c$  were so close.  $S_1$ ,  $S_2$ ,  $S_3$ ,  $S_4$  and  $S_c$  had worn rates of 14,100  $\text{mm}^3/\text{m}$ , 24,200  $\text{mm}^3/\text{m}$ , 19,500  $\text{mm}^3/\text{m}$ , 11,333  $\text{mm}^3/\text{m}$  and 16,633  $\text{mm}^3/\text{m}$  respectively.

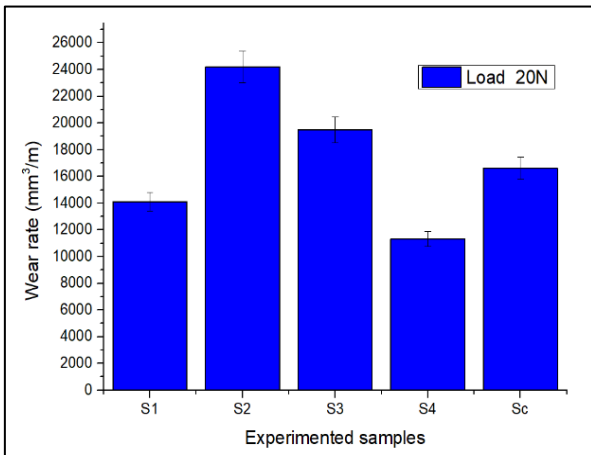


**Figure 12.** Plot of wear rate for tested samples

Figure 13 illustrates the rate of wear loss (volume loss) in each sample. From the Figure 13, sample  $S_2$  had the highest volume loss, which is the sample with (10% bamboo+5% iron-filling), while  $S_4$  had the least wear volume which is the sample with 15% iron-filling. It can be seen that there is a direct relationship between wear rate and wear volume.

It can be noticed from Figure 14 that sample  $S_4$  possessed the highest wear resistance which was the sample with 15% iron-filling. Sample  $S_1$  had a reasonable wear resistance compared to samples  $S_2$  and  $S_3$ . Sample  $S_2$  gave the least

resistance to wear which was the sample with the composition 10% bamboo and 5% iron-filling.

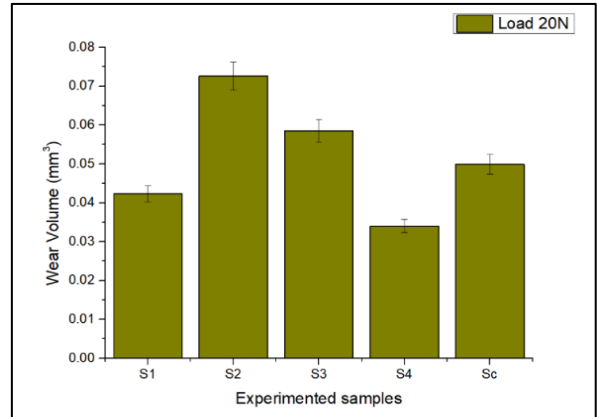


**Figure 13.** Plot of wear volume for tested samples

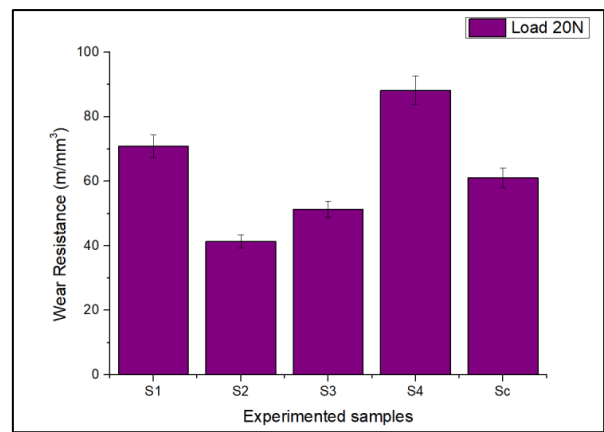


**Figure 14.** Plot of wear resistance for tested samples

Figure 15 shows the coefficient of friction for all the samples under investigation. It was noticed that the COF for all the samples fall within 0.4501 ( $S_4$ ) to 0.4909 ( $S_2$ ). All the samples have very close COF and they behave alike frictional coefficient.

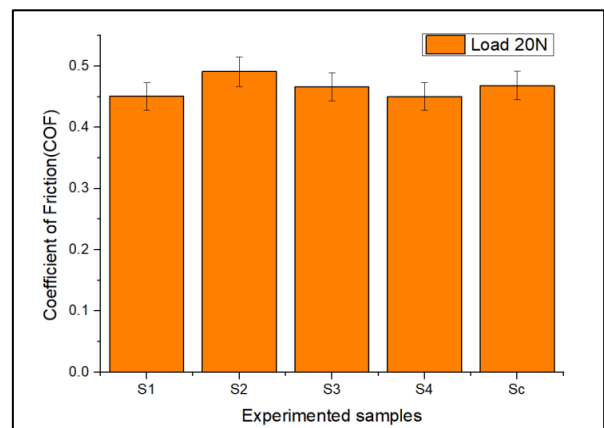


**Figure 15.** Plot of Coefficient of Friction for tested samples

The Profiler for samples  $S_1$  to  $S_c$  is presented in Figure 16 ( $S_1$ - $S_c$ ). The profiler predicted the volume loss or volume wear [16, 17, 20]. As presented in Table 6, as well as Figure 16  $S_2$ , sample  $S_4$  gave the least volume loss and sample  $S_2$  produced the highest volume loss.

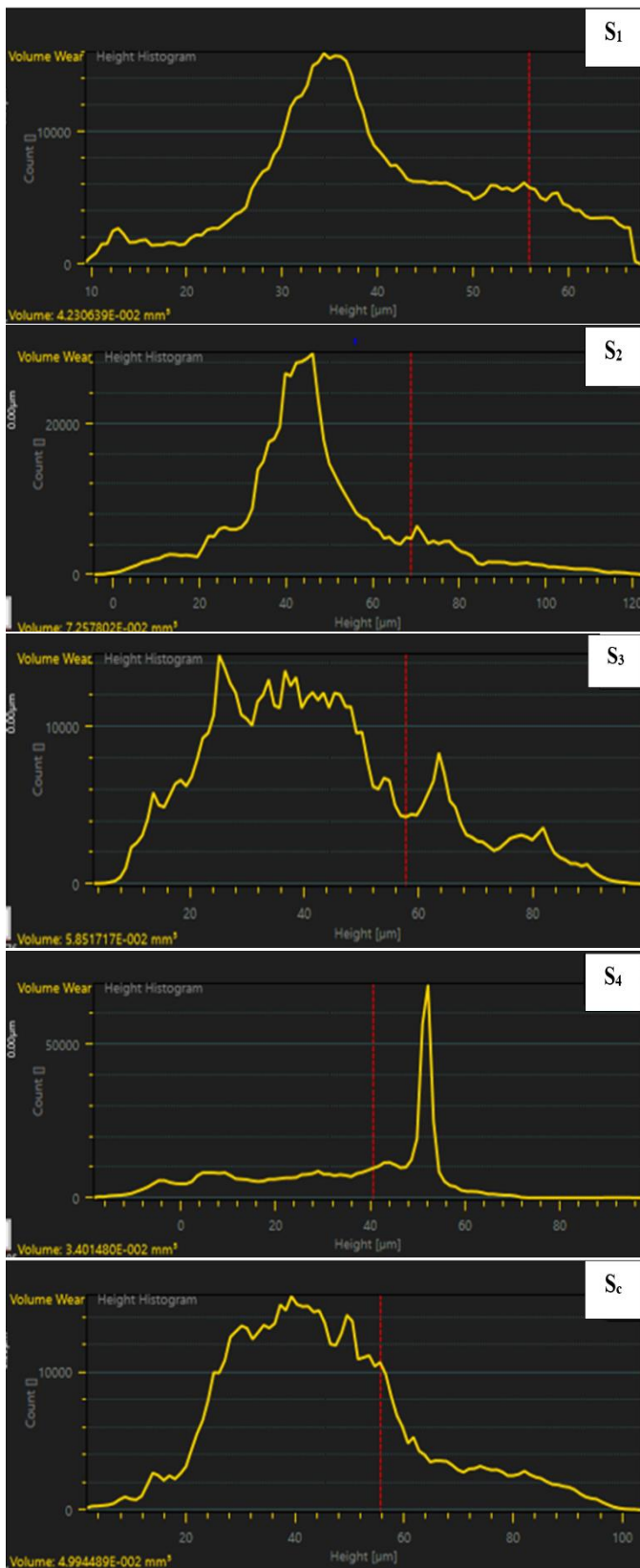


Figure 16. Profiler for samples S<sub>1</sub> to S<sub>c</sub>

#### 4. CONCLUSIONS

The mechanical properties of an AA6061 metal matrix composite, which was reinforced with bamboo powder and iron fillings, were studied and found to be satisfactory. Based on the evaluation, the following conclusions can be drawn.

1) Sample 4 containing 15% iron fillings gave the

highest value of 114.81 BHN and impact energy of 1.86 J/mm<sup>2</sup> respectively and had the lowest wear rate of 11333 mm<sup>3</sup>/m an indication that the hardness of the material was increased with the addition of iron fillings.

2) Sample 1 containing 15% bamboo powder gave the least impact strength value of 1.5 J/mm<sup>2</sup> indicating that the reinforcement material reduced the impact strength.

3) Sample 5 (control) gave the least hardness number value of 95.33 followed by sample 1 (15% bamboo powder) with 98.22 BHN due to absence of reinforcement and strength of reinforcement materials, respectively.

4) Sample 2 containing 5% iron fillings and 10% bamboo powder gave the highest wear rate of 24200 mm<sup>3</sup>/m and sample 4 (containing 15% iron fillings had the least wear rate value signifying highest wear resistance value.

#### REFERENCES

- [1] Akinwamide, S.O. (2020). Characterisation of stir-cast ferrotitanium and silicon carbide reinforced aluminium matrix composites (Doctoral Dissertation, University of Johannesburg (South Africa)). <https://doi.org/10.13140/RG.2.2.34511.82084>
- [2] Sunil, B.R., Reddy, G.P.K., Patle, H., Dumpala, R. (2016). Magnesium based surface metal matrix composites by friction stir processing. *Journal of Magnesium and Alloys*, 4(1): 52-61. <https://doi.org/10.1016/j.jma.2016.02.001>
- [3] Surappa, M.K. (2003). Aluminium matrix composites: Challenges and opportunities. *Sadhana*, 28: 319-334. <https://doi.org/10.1007/BF02717141>
- [4] Nturanabo, F., Masu, L., Kirabira, J.B. (2019). Novel applications of aluminium metal matrix composites. *Aluminium Alloys and Composites*. <https://doi.org/10.5772/intechopen.86225>
- [5] Macke, A., Schultz, B.F., Rohatgi, P. (2012). Metal matrix composites offer the automotive industry and opportunity to reduce vehicle weight. *Improve Performance. Advanced Materials & Processes*. March, 170(3): 19-23.
- [6] Adetunla, A., Adaramola, B., Ikumapayi, O., Ige, E.O., Afolalu, S. (2022). An in-depth study of magnesium composite in various corrosive media: Insight in orthopedic implant. *Journal of Composite & Advanced Materials/Revue des Composites et des Matériaux Avancés*, 32(6): 271-276. <https://doi.org/10.18280/rcma.320602>
- [7] Cheng, S.L., Yang, G.C., Man, Z., Wang, J.C., Zhou, Y.H. (2010). Mechanical properties and fracture mechanisms of aluminium matrix composites reinforced by Al<sub>9</sub>(Co, Ni)<sub>2</sub> intermetallics. *Transactions of Nonferrous Metals Society of China*, 20(4): 572-576. [https://doi.org/10.1016/S1003-6326\(09\)60180-1](https://doi.org/10.1016/S1003-6326(09)60180-1)
- [8] Ikumapayi, O.M., Afolalu, S.A., Bodunde, O.P., Ugwuoke, C.P., Benjamin, H.A., Akinlabi, E.T. (2022). Efficacy of heat treatment on the material properties of aluminium alloy matrix composite impregnated with silver nano particle/calcium carbonate Al-AgNp/CaCO<sub>3</sub>. *International Journal of Advanced Technology and Engineering Exploration*, 9(89): 523. <https://doi.org/10.19101/IJATEE.2021.874829>
- [9] Udo, M., Afolalu, S.A., Ikumapayi, O.M., Babalola, P., Obasa, V., Akpalikpo, O. (2022). Effect of particle size and weight percentage variation on the mechanical



- properties of periwinkle shell reinforced polymer (epoxy resin) matrix composite. *International Journal of Applied Science and Engineering*, 19(3): 1-7. [https://doi.org/10.6703/IJASE.202209\\_19\(3\).004](https://doi.org/10.6703/IJASE.202209_19(3).004)
- [10] Ajuka, L.O., Odunfa, M.K., Oyewola, M.O., Ikumapayi, O.M., Akinlabi, S.A., Akinlabi, E.T. (2022). Modeling of viscosity of composite of TiO<sub>2</sub>-Al<sub>2</sub>O<sub>3</sub> and ethylene glycol nanofluid by artificial neural network: Experimental correlation. *International Journal on Interactive Design and Manufacturing (IJIDeM)*, pp. 1-10. <https://doi.org/10.1007/s12008-022-00906-0>
- [11] Krishnan, P.K., Christy, J.V., Arunachalam, R., Mourad, A.H.I., Muraliraja, R., Al-Maharbi, M., Murali, V., Chandra, M.M. (2019). Production of aluminium alloy-based metal matrix composites using scrap aluminium alloy and waste materials: Influence on microstructure and mechanical properties. *Journal of Alloys and Compounds*, 784: 1047-1061. <https://doi.org/10.1016/j.jallcom.2019.01.115>
- [12] Ajuka, L.O., Ogedengbe, T.S., Adeyi, T., Ikumapayi, O.M., Akinlabi, E.T. (2023). Wear characteristics, reduction techniques and its application in automotive parts-A review. *Cogent Engineering*, 10(1): 2170741. <https://doi.org/10.1080/23311916.2023.2170741>
- [13] Ikumapayi, O., Akinlabi, E., Sharma, A., Sharma, V., Oladijo, O. (2020). Tribological, structural and mechanical characteristics of friction stir processed aluminium-based matrix composites reinforced with stainless steel micro-particles. *Engineering Solid Mechanics*, 8(3): 253-270. <http://dx.doi.org/10.5267/j.esm.2019.12.001>
- [14] Ogedengbe, T.S., Ikumapayi, O.M., Afolalu, S.A., Musa-Olokuta, A.I., Adeyi, T.A., Omovigho, M.O., Nkanga, J.B. (2022). Comparative analysis on the effect of agro-waste based flux during arc-welding of mild-steel. *Revue des Composites et des Materiaux Avances*, 32(4): 199-204. <https://doi.org/10.18280/rcma.320405>
- [15] Afolalu, S.A., Ikumapayi, O.M., Ogedengbe, T.S., Emeteri, M.E. (2021). Performance assessment of the developed flux powder on the tensile and hardness properties of steels joints using TIG-Welding. *Journal of Composite & Advanced Materials/Revue des Composites et des Materiaux Avances*, 31(3): 153-157. <https://doi.org/10.18280/rcma.310306>
- [16] Ikumapayi, O.M., Akinlabi, E.T., Majumdar, J.D., Oladijo, O.P., Akinlabi, S.A. (2019). Influence of wood fly ash reinforcement on the wear behaviour of friction stir processed aluminium-based surface matrix composite. In *Proceedings of the International Conference on Industrial Engineering and Operations Management*, 50: 966-977.
- [17] Afolalu, S.A., Abioye, A.A., Idirisu, J., Okokpuije, I.P., Ikumapayi, O.M. (2018). Abrasion wear of cutting tool developed from recycled steel using palm kernel shell as carbon additive. *Progress in Industrial Ecology, an International Journal*, 12(1-2): 206-218. <https://doi.org/10.1504/PIE.2018.095868>
- [18] Abegunde, P.O., Kazeem, R.A., Akande, I.G., Ikumapayi, O.M., Adebayo, A.S., Jen, T.C., Akinlabi, S.A., Akinlabi, E.T. (2023). Performance assessment of some selected vegetable oils as lubricants in turning of AISI 1045 steel using a Taguchi-based grey relational analysis approach. *Tribology-Materials, Surfaces & Interfaces*, 17(3): 187-202. <https://doi.org/10.1080/17515831.2023.2235227>
- [19] Afolalu, S.A., Salawu, E.Y., Okokpuije, I.P., Abioye, A.A., Abioye, O.P., Udo, M., Ikumapayi, O.M. (2017). Experimental analysis of the wear properties of carburized HSS (ASTM A600) cutting tool. *International Journal of Applied Engineering Research*, 12(19): 8995-9003.
- [20] Aladesanmi, V.I., Fatoba, O.S., Akinlabi, E.T., Ikumapayi, O.M. (2021). Analysis of wear properties and surface roughness of laser additive manufactured (LAM) Ti and TiB<sub>2</sub> metal matrix composite. *Materials Today: Proceedings*, 44: 1279-1285. <https://doi.org/10.1016/j.matpr.2020.11.266>